Variable Neural Adaptive Robust Output Feedback Control of Uncertain Systems

Jianming Lian, Wei Zhang, Jianghai Hu and Stanislaw H. Żak

***Abstract*— The design of an adaptive robust output feedback controller is presented for a class of multi-input multi-output uncertain systems. The proposed output feedback controller uses a variable-structure radial basis function (RBF) network to approximate unknown system dynamics. The output feedback implementation is realized employing a high-gain observer. The structure variation of the RBF network is taken into account in the stability analysis of the closed-loop system using the piecewise quadratic Lyapunov function. The performance of the proposed variable neural adaptive robust output feedback controller is illustrated with simulations.**

I. Introduction

Adaptive control strategies such as adaptive feedback linearization [1], adaptive backstepping [2], nonlinear damping and swapping [3], and switching adaptive control [4] have been proposed to deal with systems with unknown dynamics and/or disturbances. In particular, adaptive controllers have been developed for single-input single-output (SISO) [5]–[7] and multi-input multi-output (MIMO) [8]–[11] feedback linearizable nonlinear systems. However, the proposed controllers often require the full access of the system states, which are usually not available in practice. A possible solution the problem of inaccessible states is to use observers to estimate the system states and then use the the state estimates in the controller implementation. For example, high-gain observers have been employed in [7], [12] to design output feedback based adaptive controllers. The advantage of using high-gain observers is that the control problem can be formulated in a standard singular perturbation form and then the singular perturbation theory can be applied to analyze the closed-loop system stability. Furthermore, when the speed of the high-gain observer is sufficiently high, the performance of the output feedback controller recovers the performance of the state feedback controller [12].

Many types of function approximators have been utilized in the construction of adaptive controllers to approximate unknown system dynamics. For example, fixed-structure radial basis function (RBF) networks have been employed in [5], [7], [11]. The disadvantage of the fixed-structure RBF network is that the set of basis functions needs to be selected off-line. To overcome this problem, multilayer neural network (MLNN) based adaptive robust control strategies were proposed in [6], [8]. Although it is not required for MLNNs to choose basis functions off-line, it is still necessary to pre-determine the number of hidden neurons. On the other hand, the RBF network has a simpler structure than that of the MLNN, faster computation time and superior adaptive performance. Recently, RBF networks with dynamically adjustable structures have been proposed in the design of adaptive controllers for SISO feedback linearizable uncertain systems in [13], [14]. Such networks preserve the advantages of RBF networks and, at the same time, overcome the limitations of fixed-structure RBF networks. However, the effect of the structure variation was not considered in the stability analysis in [13], [14], where the system stability is analyzed only for each fixed structure.

In this paper, we consider the problem of output tracking control for a class of MIMO feedback linearizable uncertain systems. The same problem was also considered in [8]–[11], [15]. In [15], an adaptive robust state feedback control strategy was proposed, where a variable-structure RBF network is used to approximate unknown system dynamics. The employed variable-structure RBF network avoids selecting basis functions off-line by allocating RBFs on-line dynamically. It adds RBFs to improve the approximation accuracy and removes RBFs to prevent the network redundancy. To avoid fast switching between different structures, the dwell time requirement was introduced. However, the implementation of the proposed controller in [15] requires a direct access of the system states, which may not be feasible in practice. To overcome this restriction, we propose a variable neural adaptive robust output feedback controller. We incorporate a high-gain observer into the state feedback control strategy proposed in [15]. The structure variation of the RBF network is also considered in the stability analysis employing a piecewise quadratic Lyapunov function approach that has been widely used in the stability analysis of switched and hybrid systems [16], [17].

II. Problem Statement

A. System Description

We consider a class of uncertain systems consisting of p coupled subsystems modeled by the following equations,

$$y_i^{(n_i)} = f_i(\boldsymbol{x}) + \sum_{j=1}^{p} g_{ij}(\boldsymbol{x})u_j + d_i, \quad i = 1, \ldots, p, \qquad (1)$$

where y_i, u_i and $d_i \in \mathbb{R}$ are the output, input and disturbance of the i-th subsystem, respectively, and $f_i(\boldsymbol{x})$ and $g_{ij}(\boldsymbol{x})$ are

This work was supported by the Office of Naval Research Grant N00014-08-1-0080 and the National Science Foundation Grant CNS-0643805.

J. Lian is with the Center for Advanced Power Systems, Florida State University, Tallahassee, FL 32310, USA. lian@caps.fsu.edu.

W. Zhang is with the Department of Electrical Engineering and Computer Sciences, University of California, Berkeley, CA 94709, USA. weizhang@eecs.berkeley.edu.

J. Hu and S. H. Żak are with the School of Electrical and Computer Engineering, Purdue University, West Lafayette, IN 47907, USA. {jianghai,zak}@purdue.edu.

unknown functions with

$$\boldsymbol{x} = \left[y_1 \ \cdots \ y_1^{(n_1-1)} \ \cdots \ y_p \ \cdots \ y_p^{(n_p-1)}\right]^\top$$

being the state vector of the whole system. The disturbance d_i may depend on time t and the state vector $\boldsymbol{x}$. Let $(\boldsymbol{A}_i, \boldsymbol{b}_i)$ be the canonical controllable pair that represents a chain of n_i integrators, and let $\boldsymbol{c}_i = [1 \ 0 \ \cdots \ 0]_{1\times n_i}$, $\boldsymbol{y} = [y_1 \ \cdots \ y_p]^\top$, $\boldsymbol{u} = [u_1 \ \cdots \ u_p]^\top$ and $\boldsymbol{d} = [d_1 \ \cdots \ d_p]^\top$. The system (1) can be represented in a compact form as

$$\begin{aligned} \dot{\boldsymbol{x}} &= \boldsymbol{A}\boldsymbol{x} + \boldsymbol{B}\left(\boldsymbol{f}(\boldsymbol{x}) + \boldsymbol{G}(\boldsymbol{x})\boldsymbol{u} + \boldsymbol{d}\right) \\ \boldsymbol{y} &= \boldsymbol{C}\boldsymbol{x}, \end{aligned} \tag{2}$$

where $\boldsymbol{A} = \mathrm{diag}[\boldsymbol{A}_1 \ \cdots \ \boldsymbol{A}_p]$, $\boldsymbol{B} = \mathrm{diag}[\boldsymbol{b}_1 \ \cdots \ \boldsymbol{b}_p]$, $\boldsymbol{C} = \mathrm{diag}[\boldsymbol{c}_1 \ \cdots \ \boldsymbol{c}_p]$, $\boldsymbol{f}(\boldsymbol{x}) = [f_1(\boldsymbol{x}) \ \cdots \ f_p(\boldsymbol{x})]^\top$ and $\boldsymbol{G}(\boldsymbol{x}) = [g_{ij}(\boldsymbol{x})]_{p\times p}$. The above system is often referred to as a square system because the number of inputs is the same as the numbers of outputs. We assume that $\boldsymbol{f}(\boldsymbol{x})$ and $\boldsymbol{G}(\boldsymbol{x})$ are Lipschitz continuous vector- and matrix-valued functions of $\boldsymbol{x}$, respectively, and that $\boldsymbol{d}$ is Lipschitz continuous in $\boldsymbol{x}$ and piecewise continuous in t with $\|\boldsymbol{d}\| \le d_o$. In addition, we consider the case where the input matrix $\boldsymbol{G}(\boldsymbol{x})$ is definite with eigenvalues bounded away from zero for all $\boldsymbol{x}$ of interest. Without loss of generality, we assume that $\boldsymbol{G}(\boldsymbol{x})$ is positive definite with $\underline{g}\boldsymbol{I}_p \le \boldsymbol{G}(\boldsymbol{x}) \le \overline{g}\boldsymbol{I}_p$, where $\underline{g}$ and $\overline{g}$ are positive constants.

B. Problem Formulation and Notation

The control objective is to design a tracking, output feedback, controller so that the i-th closed-loop system output y_i, $i = 1, \ldots, p$, tracks a reference signal y_{di}, where each y_{di} has bounded derivatives up to the n_i-th order. We propose a variable-structure RBF network based adaptive robust output feedback controller. To proceed, we define the desired system state vector as $\boldsymbol{x}_d = [y_{d1} \ \cdots \ y_{d1}^{(n_1-1)} \ \cdots \ y_{dp} \ \cdots \ y_{dp}^{(n_p-1)}]^\top$ and let $\boldsymbol{y}_d^{(n)} = [y_{d1}^{(n_1)} \ \cdots \ y_{dp}^{(n_p)}]^\top$. Because the reference signal y_{di} has bounded derivatives up to the n_i-th order, we have $\boldsymbol{x}_d \in \boldsymbol{\Omega}_{x_d}$ and $\boldsymbol{y}_d^{(n)} \in \boldsymbol{\Omega}_{y_d}$, where $\boldsymbol{\Omega}_{x_d}$ and $\boldsymbol{\Omega}_{y_d}$ are compact subsets of $\mathbb{R}^n$ and $\mathbb{R}^p$, respectively, and $n = \sum_{i=1}^p n_i$. Let $e_{yi} = y_i - y_{di}$ denote the i-th output tracking error. We define the output tracking error as $\boldsymbol{e}_y = [e_{y1} \ \cdots \ e_{yp}]^\top$ and the state tracking error as $\boldsymbol{e} = \boldsymbol{x} - \boldsymbol{x}_d$. It follows from (2) that the state tracking error dynamics are modeled by

$$\dot{\boldsymbol{e}} = \boldsymbol{A}\boldsymbol{e} + \boldsymbol{B}\left(\boldsymbol{f}(\boldsymbol{x}) + \boldsymbol{G}(\boldsymbol{x})\boldsymbol{u} - \boldsymbol{y}_d^{(n)} + \boldsymbol{d}\right). \tag{3}$$

Let $\boldsymbol{K} = \mathrm{diag}[\boldsymbol{k}_1 \ \ldots \ \boldsymbol{k}_p]$ be selected such that $\boldsymbol{A}_{mi} = \boldsymbol{A}_i - \boldsymbol{b}_i\boldsymbol{k}_i$ is Hurwitz. Thus, $\boldsymbol{A}_m = \mathrm{diag}[\boldsymbol{A}_{m1} \ \cdots \ \boldsymbol{A}_{mp}]$ is Hurwitz. Let $\boldsymbol{\Omega}_{e_0}$ be a compact set that contains all possible initial state tracking errors and let $c_{e_0} = \max_{\boldsymbol{e}\in\boldsymbol{\Omega}_{e_0}} \frac{1}{2}\boldsymbol{e}^\top\boldsymbol{P}_m\boldsymbol{e}$, where $\boldsymbol{P}_m = \mathrm{diag}[\boldsymbol{P}_{m1} \ \cdots \ \boldsymbol{P}_{mp}]$ is the solution to the continuous Lyapunov matrix equation $\boldsymbol{A}_m^\top\boldsymbol{P}_m + \boldsymbol{P}_m\boldsymbol{A}_m = -2\boldsymbol{Q}_m$ for $\boldsymbol{Q}_m = \mathrm{diag}[\boldsymbol{Q}_{m1} \ \cdots \ \boldsymbol{Q}_{mp}]$ with $\boldsymbol{Q}_{mi} = \boldsymbol{Q}_{mi}^\top > 0$. Choose $c_e > c_{e_0}$ and let $\boldsymbol{\Omega}_e = \{\boldsymbol{e} : \frac{1}{2}\boldsymbol{e}^\top\boldsymbol{P}_m\boldsymbol{e} \le c_e\}$. Let $\boldsymbol{\Omega}_x = \{\boldsymbol{x} : \boldsymbol{x} = \boldsymbol{e} + \boldsymbol{x}_d, \boldsymbol{e} \in \boldsymbol{\Omega}_e, \boldsymbol{x}_d \in \boldsymbol{\Omega}_{x_d}\}$, denote the compact set over which the unknown system dynamics are approximated by a variable-structure RBF network.

III. Variable-Structure RBF Network

The variable-structure RBF network that we use to approximate unknown functions $\boldsymbol{f}(\boldsymbol{x})$ over a compact set $\boldsymbol{\Omega}_x$ is an improved version of the one proposed by us in [15]. It has N different admissible structures, where N is a design parameter. For each admissible structure, the RBF network consists of n input neurons, M_v hidden neurons, where $v \in \{1, \ldots, N\}$, and p output neurons. The k-th output of the RBF network with the v-th admissible structure can be represented as

$$\hat{f}_{k,v}(\boldsymbol{x}) = \sum_{j=1}^{M_v} \omega_{kj,v}\xi_{j,v}(\boldsymbol{x}), \tag{4}$$

where $\omega_{kj,v}$ is the weight from the j-th hidden neuron to the k-th output neuron and $\xi_{j,v}(\boldsymbol{x})$ is the radial basis function for the j-th hidden neuron. Let $\boldsymbol{W}_v = [\boldsymbol{\omega}_{1,v} \ \cdots \ \boldsymbol{\omega}_{p,v}]$ with $\boldsymbol{\omega}_{i,v} = [\omega_{i1,v} \ \cdots \ \omega_{iM_v,v}]^\top$ and $\boldsymbol{\xi}_v(\boldsymbol{x}) = [\xi_{1,v}(\boldsymbol{x}) \ \cdots \ \xi_{M_v,v}(\boldsymbol{x})]^\top$. We have $\hat{\boldsymbol{f}}_v(\boldsymbol{x}) = \boldsymbol{W}_v^\top\boldsymbol{\xi}_v(\boldsymbol{x})$, where $\hat{\boldsymbol{f}}_v(\boldsymbol{x}) = [\hat{f}_{1,v}(\boldsymbol{x}) \ \cdots \ \hat{f}_{p,v}(\boldsymbol{x})]^\top$. In this paper, we employ the same raised-cosine RBF as used in [15] instead of the commonly used Gaussian RBF.

In the following, we provide a description of the improved variable-structure RBF network. The major improvement over [15] lies in the RBF adding and removing operations.

A. Center Grid

Recall that the unknown function $\boldsymbol{f}(\boldsymbol{x})$ is approximated over a compact set $\boldsymbol{\Omega}_x \subset \mathbb{R}^n$. To locate the centers of RBFs inside the approximation region $\boldsymbol{\Omega}_x$, we utilize an n-dimensional center grid with layer hierarchy, where each grid node corresponds to the center of one RBF. The grid nodes of the center grid are located at $S_1 \times \cdots \times S_n$, where S_i is the set of locations of the grid nodes in the i-th coordinate and $\times$ denotes the Cartesian product. The center grid is initialized inside the approximation region $\boldsymbol{\Omega}_x$ with $S_i = \{x_{li}, x_{ui}\}$, $i = 1, \ldots, n$, where x_{li} and x_{ui} denote the lower and upper bounds in the i-th coordinate. The 2^n grid nodes of the initial grid are referred to as the boundary grid nodes, and they are non-removable.

B. Adding RBFs

If the time elapsed since the last operation of adding or removing is greater than the dwell time T_d, and $\|\boldsymbol{e}_y\| > e_{\max}$, where $e_{\max}$ is a prespecified design parameter, for a period of time greater than T_d, then the network attempts to add new RBFs represented by some new grid nodes. First, the nearest neighboring grid node in the center grid, denoted $\boldsymbol{c}_{(\mathrm{nearest})}$, to the current input $\boldsymbol{x}$ is located among existing grid nodes. Then the "nearer" neighboring grid node in the center grid denoted $\boldsymbol{c}_{(\mathrm{nearer})}$ is located, where $c_{i(\mathrm{nearer})}$ is determined so that x_i is between $c_{i(\mathrm{nearest})}$ and $c_{i(\mathrm{nearer})}$. The adding operation is performed for each coordinate independently. In the i-th coordinate, if the following conditions are satisfied:

(1) $\left|x_i - c_{i(\mathrm{nearest})}\right| > \frac{1}{4}\left|c_{i(\mathrm{nearest})} - c_{i(\mathrm{nearer})}\right|$,
(2) $\left|x_i - c_{i(\mathrm{nearest})}\right| > d_{i(\mathrm{threshold})}$,

where $d_{i(\text{threshold})}$ is a design parameter that specifies the minimum grid distance in the i-th coordinate and thus determines the number of admissible structures denoted by N, then a new location at exactly the middle of $c_{i(\text{nearest})}$ and $c_{i(\text{nearer})}$ is added into S_i. Otherwise, no new location is added to S_i. The layer of the newly added location is one level higher than the highest layer of the two adjacent existing locations in the same coordinate.

C. Removing RBFs

If the elapsed time since the last operation of adding or removing is greater than the dwell time T_d, and $\|\boldsymbol{e}_y\| \leq \rho e_{\max}$, where $\rho \in (0,\ 1]$, for a period of time greater than T_d, then the network attempts to remove some of the existing RBFs, that is, some of the existing grid nodes, to prevent network redundancy. The RBF removing operation is also implemented for each coordinate independently. In the i-th coordinate, if the following conditions are satisfied:

(1) $c_{i(\text{nearest})} \notin \{x_{li}, x_{ui}\}$,
(2) the location $c_{i(\text{nearest})}$ is in the higher than or in the same layer as the highest layer of the two neighboring locations in the same coordinate,
(3) $\left|x_i - c_{i(\text{nearest})}\right| < \varrho \left|c_{i(\text{nearest})} - c_{i(\text{nearer})}\right|$, $\varrho \in (0,\ 0.5)$,

then the location $c_{i(\text{nearest})}$ is removed from S_i. Otherwise, no location is removed from S_i.

D. Uniform Grid Transformation

The determination of the radius of the RBF is achieved by uniform grid transformation, whose details can be found in [15]. When implementing the output feedback controller, the state vector estimate, $\hat{\boldsymbol{x}}$, is used rather than the actual state vector, $\boldsymbol{x}$. The case when $\hat{\boldsymbol{x}} \notin \boldsymbol{\Omega}_x$ is analyzed in detail in [14].

IV. High-Gain Tracking Error Observer

We assume that the system states are not available for the feedback implementation. Thus, we apply the high-gain observer, as in [7], [12],

$$\dot{\hat{\boldsymbol{e}}}_i = \boldsymbol{A}_i \hat{\boldsymbol{e}}_i + \boldsymbol{l}_i \left(e_{yi} - \boldsymbol{c}_i \hat{\boldsymbol{e}}_i\right), \quad i = 1, \ldots, p \tag{5}$$

to estimate the tracking error $\boldsymbol{e}_i$ of the i-th subsystem. The observer gain $\boldsymbol{l}_i$ is chosen as $\boldsymbol{l}_i = [\alpha_{i1}/\epsilon \ \cdots \ \alpha_{in_i}/\epsilon^{n_i}]^\top$, where $\epsilon \in (0,1)$ is a design parameter and α_{ij}, $j = 1, \ldots, n_i$, are selected so that the roots of the characteristic polynomial equation, $s^{n_i} + \alpha_{i1} s^{n_i - 1} + \cdots + \alpha_{i(n_i-1)} s + \alpha_{in_i} = 0$, have negative real parts. Let $\hat{\boldsymbol{e}} = [\hat{\boldsymbol{e}}_1^\top \ \cdots \ \hat{\boldsymbol{e}}_p^\top]^\top$ and $\boldsymbol{L} = \operatorname{diag}[\boldsymbol{l}_1 \ \cdots \ \boldsymbol{l}_p]$. Then the high-gain observer (5) can be represented as

$$\dot{\hat{\boldsymbol{e}}} = \boldsymbol{A}\hat{\boldsymbol{e}} + \boldsymbol{L}\left(\boldsymbol{e}_y - \boldsymbol{C}\hat{\boldsymbol{e}}\right). \tag{6}$$

To facilitate stability analysis of the closed-loop system, we represent the estimation error dynamics in the singularly perturbed form. Let $\boldsymbol{\zeta} = [\boldsymbol{\zeta}_1^\top \ \cdots \ \boldsymbol{\zeta}_p^\top]^\top$, where $\boldsymbol{\zeta}_i = [\zeta_{i1} \ \cdots \ \zeta_{in_i}]^\top$ with

$$\zeta_{ij} = \frac{e_{yi}^{(j-1)} - \hat{e}_{yi}^{(j-1)}}{\epsilon^{n_i - j}}, \quad j = 1, \ldots, n_i. \tag{7}$$

It follows from (7) that $\hat{\boldsymbol{e}} = \boldsymbol{e} - \boldsymbol{D}\boldsymbol{\zeta}$, where $\boldsymbol{D} = \operatorname{diag}[\boldsymbol{D}_1 \ \cdots \ \boldsymbol{D}_p]$ and $\boldsymbol{D}_i = \operatorname{diag}[\epsilon^{n_i - 1} \ \cdots \ 1]$. Note that $\|\boldsymbol{D}\| = 1$. Combining (3), (6) and (7) yields

$$\epsilon \dot{\boldsymbol{\zeta}} = \boldsymbol{A}_c \boldsymbol{\zeta} + \epsilon \boldsymbol{B}\left(\boldsymbol{f}(\boldsymbol{x}) + \boldsymbol{G}(\boldsymbol{x})\boldsymbol{u} - \boldsymbol{y}_d^{(n)} + \boldsymbol{d}\right), \tag{8}$$

where $\boldsymbol{A}_c = \operatorname{diag}[\boldsymbol{A}_{c1} \ \cdots \ \boldsymbol{A}_{cp}]$ and $\boldsymbol{A}_{ci} = \epsilon \boldsymbol{D}_i^{-1}(\boldsymbol{A}_i - \boldsymbol{l}_i \boldsymbol{c}_i)\boldsymbol{D}_i$ is a Hurwitz matrix. Applying the method of [18], we can prove the following proposition.

Proposition 1: Suppose that the control input $\boldsymbol{u}$ is globally bounded. There exists a constant $\epsilon_1^* \in (0,1)$ such that if $\epsilon \in (0, \epsilon_1^*)$, then $\|\boldsymbol{\zeta}(t)\| \leq \beta\epsilon$ with some $\beta > 0$ for $t \in [t_0 + T_1(\epsilon), t_0 + T_3)$, where $T_1(\epsilon)$ is a finite time and $t_0 + T_3$ is the moment when the tracking error $\boldsymbol{e}(t)$ leaves the compact set $\boldsymbol{\Omega}_e$ for the first time. Moreover, we have $\lim_{\epsilon \to 0^+} T_1(\epsilon) = 0$ and $c_{e_1} = \frac{1}{2}\boldsymbol{e}(t_0 + T_1(\epsilon))^\top \boldsymbol{P}_m \boldsymbol{e}(t_0 + T_1(\epsilon)) < c_e$.

We define the estimate of the system state vector $\boldsymbol{x}$ as $\hat{\boldsymbol{x}} = \boldsymbol{x}_d + \hat{\boldsymbol{e}}$. In the following Section, we present the design of the proposed variable neural adaptive robust output feedback controller.

V. Output Feedback Controller

A. Controller Structure

We consider adaptive robust output feedback controller,

$$\begin{aligned}\hat{\boldsymbol{u}} &= \hat{\boldsymbol{u}}_{a,v} + \hat{\boldsymbol{u}}_{s,v} \\ &= \boldsymbol{G}_0^{-1}\left(-\hat{\boldsymbol{f}}_v(\hat{\boldsymbol{x}}) + \boldsymbol{y}_d^{(n)} - \boldsymbol{K}\hat{\boldsymbol{e}}\right) + \hat{\boldsymbol{u}}_{s,v},\end{aligned} \tag{9}$$

where $\boldsymbol{G}_0$ is a chosen positive definite matrix, $\hat{\boldsymbol{f}}_v(\hat{\boldsymbol{x}}) = \boldsymbol{W}_v^\top \boldsymbol{\xi}_v(\hat{\boldsymbol{x}})$, and $\hat{\boldsymbol{u}}_{s,v}$ is the robustifying component to be designed later. It is obvious that the controller architecture varies as the structure of the RBF network changes. Hence, the controller has N different architectures, which are referred to as *modes*.

To proceed, recall that $\boldsymbol{W}_v = [\boldsymbol{\omega}_{1,v} \ \cdots \ \boldsymbol{\omega}_{p,v}]$. We constrain the weight vectors $\boldsymbol{\omega}_{i,v}$ to reside in the compact sets $\boldsymbol{\Omega}_{i,v} = \{\boldsymbol{\omega}_{i,v} : \underline{\omega}_i \leq \omega_{ij,v} \leq \overline{\omega}_i, 1 \leq j \leq M_v\}$, where $\underline{\omega}_i$ and $\overline{\omega}_i$, $i = 1, \ldots, p$, are design parameters. Let $\boldsymbol{W}_v^* = [\boldsymbol{\omega}_{1,v}^* \ \cdots \ \boldsymbol{\omega}_{p,v}^*]$ denote the "optimal" constant weight matrix corresponding to the v-th network structure, that is,

$$\boldsymbol{W}_v^* = \operatorname*{argmin}_{\boldsymbol{\omega}_{i,v} \in \boldsymbol{\Omega}_{i,v}} \max_{\boldsymbol{x} \in \boldsymbol{\Omega}_x} \left\|\boldsymbol{f}(\boldsymbol{x}) - \boldsymbol{W}_v^\top \boldsymbol{\xi}_v(\boldsymbol{x})\right\|.$$

Note that this $\boldsymbol{W}_v^*$ is used only for analytical purpose. Let $\boldsymbol{\Phi}_v = \boldsymbol{W}_v - \boldsymbol{W}_v^* = [\boldsymbol{\phi}_{1,v} \ \cdots \ \boldsymbol{\phi}_{p,v}]$ with $\boldsymbol{\phi}_{i,v} = \boldsymbol{\omega}_{i,v} - \boldsymbol{\omega}_{i,v}^*$, and let $c = \sum_{i=1}^p c_i$, where

$$c_i = \max_v \left(\max_{\boldsymbol{\omega}_{i,v}, \boldsymbol{\omega}_{i,v}^* \in \boldsymbol{\Omega}_{i,v}} \frac{1}{2\kappa}\boldsymbol{\phi}_{i,v}^\top \boldsymbol{\phi}_{i,v}\right), \tag{10}$$

where $\kappa > 0$ is a design parameter, and $\max_v(\cdot)$ denotes the maximization taken over all the admissible structures of the RBF networks. It is obvious that c_i decreases as κ increases. Let $\hat{\boldsymbol{\sigma}} = \boldsymbol{B}^\top \boldsymbol{P}_m \hat{\boldsymbol{e}}$. The following projection based weight matrix adaptation law is employed,

$$\dot{\boldsymbol{W}}_v = \operatorname{Proj}\left(\boldsymbol{W}_v, \kappa \boldsymbol{\xi}_v(\hat{\boldsymbol{x}})\hat{\boldsymbol{\sigma}}^\top\right), \tag{11}$$

where $\mathrm{Proj}(\boldsymbol{W}_v, \boldsymbol{\Theta}_v)$ denotes $\mathrm{Proj}(\omega_{ij,v}, \theta_{ij,v})$ for $i = 1, \ldots, p$ and $j = 1, \ldots, M_v$ and $\mathrm{Proj}(\omega_{ij,v}, \theta_{ij,v})$ is the discontinuous projection operator used in [14]. It is easy to verify that

$$\frac{1}{\kappa} \operatorname{trace}\left(\boldsymbol{\Phi}_v^\top \left(\dot{\boldsymbol{W}}_v - \kappa \boldsymbol{\xi}_v(\hat{\boldsymbol{x}}) \hat{\boldsymbol{\sigma}}^\top\right)\right) \leq 0. \tag{12}$$

Choose two positive constants d_f and d_g such that

$$d_f \geq d_f^* = \max_v \left(\max_{\boldsymbol{x} \in \boldsymbol{\Omega}_x} \left\| \boldsymbol{f}(\boldsymbol{x}) - \boldsymbol{W}_v^{*\top} \boldsymbol{\xi}_v(\boldsymbol{x}) \right\| \right)$$

and $d_g \geq d_g^* = \max_{\boldsymbol{x} \in \boldsymbol{\Omega}_x} \|\boldsymbol{G}(\boldsymbol{x}) - \boldsymbol{G}_0\|$. Then we propose to use in (9) the robustifying component $\hat{\boldsymbol{u}}_{s,v}$ of the form,

$$\hat{\boldsymbol{u}}_{s,v} = \begin{cases} -\dfrac{\hat{k}_{s,v}}{\underline{g}} \dfrac{\hat{\boldsymbol{\sigma}}}{\|\hat{\boldsymbol{\sigma}}\|} & \text{if } \|\hat{\boldsymbol{\sigma}}\| \geq \nu \\ -\dfrac{\hat{k}_{s,v}}{\underline{g}} \dfrac{\hat{\boldsymbol{\sigma}}}{\nu} & \text{if } \|\hat{\boldsymbol{\sigma}}\| < \nu, \end{cases}$$

where $\hat{k}_{s,v} = d_f + d_g \|\hat{\boldsymbol{u}}_{a,v}\| + d_o$ and $\nu > 0$ is a design parameter.

Recall that there exist peaking phenomena [19] associated with the high-gain observer described by (6). Thus, we cannot directly apply the output feedback controller given by (9). To eliminate the peaking phenomena, we introduce saturation to the control input (9). Let $\boldsymbol{\Omega}_{\hat{e}} = \left\{\boldsymbol{e} : \frac{1}{2}\boldsymbol{e}^\top \boldsymbol{P}_m \boldsymbol{e} \leq c_{\hat{e}}\right\}$, where $c_{\hat{e}} > c_e$. Let $\boldsymbol{u}$ denote the state feedback controller obtained by replacing $\hat{\boldsymbol{x}}$ with $\boldsymbol{x}$ in (9), and let $U_i \geq \max_v(\max|u_i(\boldsymbol{e}, \boldsymbol{x}_d, \boldsymbol{y}_{di}^{(n)}, \boldsymbol{\omega}_{i,v})|)$, where u_i is the i-th element of $\boldsymbol{u}$ and the inner maximization is taken over $\boldsymbol{e} \in \boldsymbol{\Omega}_{\hat{e}}$, $\boldsymbol{x}_d \in \boldsymbol{\Omega}_{x_d}$, $\boldsymbol{y}_{di}^{(n)} \in \Omega_{y_{di}}$ and $\boldsymbol{\omega}_{i,v} \in \boldsymbol{\Omega}_{i,v}$. Then the proposed adaptive robust output feedback controller takes the form

$$\boldsymbol{u}^s = \left[U_1 \operatorname{sat}\left(\frac{\hat{u}_1}{U_1}\right) \cdots U_p \operatorname{sat}\left(\frac{\hat{u}_p}{U_p}\right)\right]^\top, \tag{13}$$

where sat is the saturation operator.

Remark 1: The existence of a unique solution to (2) with the proposed variable neural adaptive robust output feedback controller can be established using the arguments of [15].

B. Stability Analysis

Note that the control input $\boldsymbol{u}^s$ is globally bounded by construction. It follows from Proposition 1 that if $\epsilon \in (0, \epsilon_1^*)$, then $\boldsymbol{e}(t) \in \boldsymbol{\Omega}_e$ and $\|\boldsymbol{\zeta}(t)\| \leq \beta\epsilon$ for $t \in [t_0 + T_1(\epsilon), t_0 + T_3)$. Thus, we have $\|\boldsymbol{e}(t) - \hat{\boldsymbol{e}}(t)\| \leq \|\boldsymbol{D}\| \|\boldsymbol{\zeta}(t)\| \leq \beta\epsilon$ for $t \in [t_0 + T_1(\epsilon), t_0 + T_3)$. There exists a constant ϵ_2 such that $\|\boldsymbol{e}(t) - \hat{\boldsymbol{e}}(t)\| \leq \beta\epsilon_2$, which implies $\hat{\boldsymbol{e}}(t) \in \boldsymbol{\Omega}_{\hat{e}}$. Let $\epsilon_2^* = \min\{\epsilon_1^*, \epsilon_2\}$. If $\epsilon \in (0, \epsilon_2^*)$, then the adaptive robust output feedback (13) is not in the saturated mode, that is, $\boldsymbol{u}^s = \hat{\boldsymbol{u}} = \hat{\boldsymbol{u}}_{a,v} + \hat{\boldsymbol{u}}_{s,v}$ for $t \in [t_0 + T_1(\epsilon), t_0 + T_3)$. Substituting $\boldsymbol{u}^s = \hat{\boldsymbol{u}}_{a,v} + \hat{\boldsymbol{u}}_{s,v}$ into the state tracking error dynamics (3) gives

$$\begin{aligned} \dot{\boldsymbol{e}} &= \boldsymbol{A}\boldsymbol{e} + \boldsymbol{B}\left(\boldsymbol{f}(\boldsymbol{x}) + \boldsymbol{G}(\boldsymbol{x})\left(\hat{\boldsymbol{u}}_{a,v} + \hat{\boldsymbol{u}}_{s,v}\right) - \boldsymbol{y}_d^{(n)} + \boldsymbol{d}\right) \\ &= \boldsymbol{A}_m \boldsymbol{e} + \boldsymbol{B}\boldsymbol{K}(\boldsymbol{e} - \hat{\boldsymbol{e}}) + \boldsymbol{B}\boldsymbol{G}(\boldsymbol{x})\hat{\boldsymbol{u}}_{s,v} + \boldsymbol{B}\boldsymbol{d} \\ &\quad + \boldsymbol{B}\left(\boldsymbol{f}(\boldsymbol{x}) - \hat{\boldsymbol{f}}_v(\hat{\boldsymbol{x}})\right) + \boldsymbol{B}\left(\boldsymbol{G}(\boldsymbol{x}) - \boldsymbol{G}_0\right)\hat{\boldsymbol{u}}_{a,v}. \end{aligned} \tag{14}$$

Now we consider the piecewise quadratic Lyapunov function candidate

$$V_v = \frac{1}{2}\boldsymbol{e}^\top \boldsymbol{P}_m \boldsymbol{e} + \frac{1}{2\kappa} \operatorname{trace}\left(\boldsymbol{\Phi}_v^\top \boldsymbol{\Phi}_v\right) \tag{15}$$

for $t \in [t_0 + T_1(\epsilon), t_0 + T_3)$ and $\epsilon \in (0, \epsilon_2^*)$, whenever the proposed adaptive robust controller (9) is in the v-th mode. It follows from (10) that

$$\frac{1}{2\kappa} \operatorname{trace}\left(\boldsymbol{\Phi}_v^\top \boldsymbol{\Phi}_v\right) = \sum_{i=1}^{p} \frac{1}{2\kappa} \boldsymbol{\phi}_{i,v}^\top \boldsymbol{\phi}_{i,v} \leq \sum_{i=1}^{p} c_i = c. \tag{16}$$

This Lyapunov function has jump discontinuities when the proposed adaptive robust output feedback controller switches between different modes. The time derivative of V_v evaluated along the solutions of (14) is

$$\begin{aligned} \dot{V}_v &= \boldsymbol{e}^\top \boldsymbol{P}_m \dot{\boldsymbol{e}} + \frac{1}{\kappa} \operatorname{trace}\left(\boldsymbol{\Phi}_v^\top \dot{\boldsymbol{\Phi}}_v\right) \\ &= -\boldsymbol{e}^\top \boldsymbol{Q}_m \boldsymbol{e} + \boldsymbol{\sigma}^\top \boldsymbol{K}(\boldsymbol{e} - \hat{\boldsymbol{e}}) + \hat{\boldsymbol{\sigma}}^\top \boldsymbol{G}(\boldsymbol{x})\hat{\boldsymbol{u}}_{s,v} \\ &\quad + \frac{1}{\kappa} \operatorname{trace}\left(\boldsymbol{\Phi}_v^\top \left(\dot{\boldsymbol{W}}_v - \kappa \boldsymbol{\xi}_v(\hat{\boldsymbol{x}})\hat{\boldsymbol{\sigma}}^\top\right)\right) + \hat{\boldsymbol{\sigma}}\boldsymbol{d} \\ &\quad + \hat{\boldsymbol{\sigma}}^\top \left(\boldsymbol{f}(\boldsymbol{x}) - \boldsymbol{W}_v^{*\top} \boldsymbol{\xi}_v(\hat{\boldsymbol{x}})\right) + (\boldsymbol{\sigma} - \hat{\boldsymbol{\sigma}})^\top \boldsymbol{d} \\ &\quad + \hat{\boldsymbol{\sigma}}^\top \left(\boldsymbol{G}(\boldsymbol{x}) - \boldsymbol{G}_0\right)\hat{\boldsymbol{u}}_{a,v} + (\boldsymbol{\sigma} - \hat{\boldsymbol{\sigma}})^\top \boldsymbol{G}(\boldsymbol{x})\hat{\boldsymbol{u}}_{s,v} \\ &\quad + (\boldsymbol{\sigma} - \hat{\boldsymbol{\sigma}})^\top \left(\boldsymbol{f}(\boldsymbol{x}) - \hat{\boldsymbol{f}}_v(\hat{\boldsymbol{x}})\right) \\ &\quad + (\boldsymbol{\sigma} - \hat{\boldsymbol{\sigma}})^\top \left(\boldsymbol{G}(\boldsymbol{x}) - \boldsymbol{G}_0\right)\hat{\boldsymbol{u}}_{a,v}. \end{aligned} \tag{17}$$

For $t \in [t_0 + T_1(\epsilon), t_0 + T_3)$, if $\epsilon \in (0, \epsilon_2^*)$, then $\|\boldsymbol{\zeta}(t)\| \leq \beta\epsilon$, $\|\boldsymbol{e}(t) - \hat{\boldsymbol{e}}(t)\| \leq \beta\epsilon$, $\boldsymbol{e}(t) \in \boldsymbol{\Omega}_e$, $\hat{\boldsymbol{e}}(t) \in \boldsymbol{\Omega}_{\hat{e}}$, $\boldsymbol{x}_d(t) \in \boldsymbol{\Omega}_{x_d}$ and $\boldsymbol{y}_d^{(n)}(t) \in \boldsymbol{\Omega}_{y_d}$. Hence, $\boldsymbol{\sigma}(t)$, $\hat{\boldsymbol{\sigma}}(t)$, $\boldsymbol{x}(t)$, $\hat{\boldsymbol{x}}(t)$, $\hat{\boldsymbol{u}}_{a,v}(t)$ and $\hat{\boldsymbol{u}}_{s,v}(t)$ are all bounded for $t \in [t_0 + T_1(\epsilon), t_0 + T_3)$. Thus, we have

$$\|\boldsymbol{\sigma}\boldsymbol{K}(\boldsymbol{e} - \hat{\boldsymbol{e}})\| \leq r_1 \epsilon \tag{18}$$

and

$$\begin{aligned} &\Big\| (\boldsymbol{\sigma} - \hat{\boldsymbol{\sigma}})^\top \left(\boldsymbol{f}(\boldsymbol{x}) - \hat{\boldsymbol{f}}_v(\hat{\boldsymbol{x}})\right) \\ &\quad + (\boldsymbol{\sigma} - \hat{\boldsymbol{\sigma}})^\top \left(\boldsymbol{G}(\boldsymbol{x}) - \boldsymbol{G}_0\right)\hat{\boldsymbol{u}}_{a,v} \\ &\quad + (\boldsymbol{\sigma} - \hat{\boldsymbol{\sigma}})^\top \left(\boldsymbol{d} + \boldsymbol{G}(\boldsymbol{x})\hat{\boldsymbol{u}}_{s,v}\right) \Big\| \leq r_2 \epsilon \end{aligned} \tag{19}$$

for some r_1, $r_2 > 0$. On the other hand, it follows from the Lipschitz continuity of the raised-cosine RBF that

$$\left\| \boldsymbol{W}_v^{*\top} \boldsymbol{\xi}_v(\boldsymbol{x}) - \boldsymbol{W}_v^{*\top} \boldsymbol{\xi}_v(\hat{\boldsymbol{x}}) \right\| \leq L_v \|\boldsymbol{x} - \hat{\boldsymbol{x}}\|$$

for some $L_v > 0$. Let $L = \max_v L_v$. Taking into account that $\|\boldsymbol{x} - \hat{\boldsymbol{x}}\| = \|\boldsymbol{e} - \hat{\boldsymbol{e}}\|$ gives

$$\begin{aligned} &\left\| \hat{\boldsymbol{\sigma}}^\top \left(\boldsymbol{f}(\boldsymbol{x}) - \boldsymbol{W}_v^{*\top} \boldsymbol{\xi}_v(\hat{\boldsymbol{x}})\right) \right\| \\ &\quad \leq \left\| \boldsymbol{f}(\boldsymbol{x}) - \boldsymbol{W}_v^{*\top} \boldsymbol{\xi}_v(\boldsymbol{x}) \right\| \|\hat{\boldsymbol{\sigma}}\| \\ &\qquad + \left\| \boldsymbol{W}_v^{*\top} \boldsymbol{\xi}_v(\boldsymbol{x}) - \boldsymbol{W}_v^{*\top} \boldsymbol{\xi}_v(\hat{\boldsymbol{x}}) \right\| \|\hat{\boldsymbol{\sigma}}\| \\ &\quad \leq d_f^* \|\hat{\boldsymbol{\sigma}}\| + L\|\boldsymbol{e} - \hat{\boldsymbol{e}}\| \|\hat{\boldsymbol{\sigma}}\| \\ &\quad \leq d_f^* \|\hat{\boldsymbol{\sigma}}\| + r_3 \epsilon \end{aligned} \tag{20}$$

for some $r_3 > 0$. It follows from (12) and (17)–(20) that

$$\dot{V}_v \leq -\boldsymbol{e}^\top \boldsymbol{Q}_m \boldsymbol{e} + \hat{k}_{s,v}^* \|\hat{\boldsymbol{\sigma}}\| + \hat{\boldsymbol{\sigma}}^\top \boldsymbol{G}(\boldsymbol{x})\hat{\boldsymbol{u}}_{s,v} + r\epsilon, \tag{21}$$

where $r = r_1+r_2+r_3$ and $\hat{k}^*_{s,v} = d^*_f+d^*_g\|\hat{\boldsymbol{u}}_{a,v}\|+d_o \le \hat{k}_{s,v}$. If $\|\hat{\boldsymbol{\sigma}}\| > \nu$, then

$$\hat{k}_{s,v}*\|\hat{\boldsymbol{\sigma}}\|+\hat{\boldsymbol{\sigma}}^\top \boldsymbol{G}(\boldsymbol{x})\hat{\boldsymbol{u}}_{s,v} \le \hat{k}_{s,v}*\|\hat{\boldsymbol{\sigma}}\|-\hat{k}_{s,v}\|\hat{\boldsymbol{\sigma}}\| \le 0. \quad (22)$$

On the other hand, if $\|\hat{\boldsymbol{\sigma}}\| \le \nu$, then

$$\hat{k}^*_{s,v}\|\hat{\boldsymbol{\sigma}}\| + \hat{\boldsymbol{\sigma}}^\top \boldsymbol{G}(\boldsymbol{x})\hat{\boldsymbol{u}}_{s,v} \le \hat{k}^*_{s,v}\|\hat{\boldsymbol{\sigma}}\| - \hat{k}^*_{s,v}\frac{\|\hat{\boldsymbol{\sigma}}\|^2}{\nu} \le \frac{\hat{k}^*_{s,v}}{4}\nu. \quad (23)$$

Combining (22) and (23), we obtain

$$\hat{k}^*_{s,v}\|\hat{\boldsymbol{\sigma}}\| + \hat{\boldsymbol{\sigma}}^\top \boldsymbol{G}(\boldsymbol{x})\hat{\boldsymbol{u}}^*_{s,v} \le \frac{\hat{k}^*_{s,v}}{4}\nu \le \frac{\hat{k}^*_s}{4}\nu, \quad (24)$$

where $\hat{k}^*_s = d^*_f + d^*_g \max_v (\max \|\hat{\boldsymbol{u}}_{a,v}\|) + d_o$ and the inner maximization is taken over $\boldsymbol{x}_d \in \boldsymbol{\Omega}_{x_d}$, $\boldsymbol{y}^{(n)}_d \in \boldsymbol{\Omega}_{y_d}$, and $\hat{\boldsymbol{e}} \in \boldsymbol{\Omega}_{\hat{e}}$. It follows from (16), (21) and (24) that

$$\begin{aligned}\dot{V}_v &\le -\boldsymbol{e}^\top \boldsymbol{Q}_m \boldsymbol{e} + \frac{\hat{k}^*_s}{4}\nu + r\epsilon \\ &\le -2\mu_m V_v + 2\mu_m c + \frac{\hat{k}^*_s}{4}\nu + r\epsilon \\ &= -\mu_m V_v - \mu_m \left(V_v - 2\hat{c} - r\epsilon\right), \end{aligned} \quad (25)$$

where $\hat{c} = c+\hat{k}^*_s\nu/(8\mu_m)$. Let $t_{0,v}$ and $t_{f,v}$ denote the initial and the final time instant, respectively, of a continuous time period when the controller is in the v-th mode. It follows from (21) that if $V_v(t) \ge 2\hat{c} + r\epsilon$ for $t \in [t_{0,v}, t_{f,v}] \cap [t_0 + T_1(\epsilon), t_0 + T_3)$, then $\dot{V}_v(t) \le -\mu_m V_v(t)$, which implies that

$$V_v(t) \le \exp(-\mu_m(t - t_{0,v}))V_v(t_{0,v}) \quad (26)$$

for $t \in [t_{0,v}, t_{f,v}] \cap [t_0 + T_1(\epsilon), t_0 + T_3)$.

Theorem 1: Let t_1, t_2 and t_3 be three consecutive switching time instants in the interval $[t_0 + T_1(\epsilon), t_0 + T_3)$ so that $v = v_1$ for $t \in [t_1, t_2]$ and $v = v_2$ for $t \in [t_2, t_3]$. Suppose that $V_v(t)$ satisfies (26) and $V_v(t) \ge 2\hat{c} + r\epsilon$ for $t \in [t_1, t_3]$. If the dwell time T_d of the variable-structure RBF network satisfies that

$$T_d \ge \frac{1}{\mu_m} \ln\left(\frac{3}{2}\right), \quad (27)$$

then $V_{v_2}(t_2) < V_{v_1}(t_1)$ and $V_{v_2}(t_3) < V_{v_1}(t_2)$.

Proof: This can be proved by replacing $2\bar{c}$ with $2\hat{c}+r\epsilon$ in the proof of Theorem 1 in [15]. ■

Theorem 2: For the system (2) driven by the proposed adaptive robust output controller (13) with the adaptation laws (11), suppose that T_d satisfies the condition (27). If $c_e \ge c_{e_1} + c$ and $c_e > 2\hat{c} + c$, there exists a constant $\epsilon^* \in (0, 1)$ so that if $\epsilon \in (0, \epsilon^*)$, then $\boldsymbol{e}(t) \in \boldsymbol{\Omega}_e$ and $\boldsymbol{x}(t) \in \boldsymbol{\Omega}_x$ for $t \ge t_0$. Moreover, there exists a finite time $T \ge t_0+T_1(\epsilon)$ such that

$$\frac{1}{2}\boldsymbol{e}(t)^\top \boldsymbol{P}_m \boldsymbol{e}(t) \le 2\hat{c} + r\epsilon + c \quad (28)$$

with some $r > 0$ for $t \ge T$. In addition, suppose that there exists a finite time $T_s \ge t_0 + T_1(\epsilon)$ such that $v = v_s$ for $t \ge T_s$. Then a finite time $T \ge T_s$ can be found such that

$$\frac{1}{2}\boldsymbol{e}^\top(t)\boldsymbol{P}_m \boldsymbol{e}(t) \le 2\hat{c} + r\epsilon \quad (29)$$

for $t \ge T$.

Proof: Recall that if $\epsilon \in (0, \epsilon^*_2)$, then $\dot{V}_v(t)$ satisfies (25) for $t \in [t_0+T_1(\epsilon), t_0+T_3)$, where we have $V(t_0+T_1(\epsilon)) \le c_{e_1} + c$. If, at the same time, T_d satisfies the condition (27), it follows from Theorem 1 that

$$\begin{aligned}V_v(t) &\le \max\left\{V(t_0 + T_1(\epsilon)), 2\hat{c} + r\epsilon + c\right\} \\ &\le \max\left\{c_{e_1} + c, 2\hat{c} + r\epsilon + c\right\}, \end{aligned} \quad (30)$$

for $t \in [t_0 + T_1(\epsilon), t_0 + T_3)$. If $c_e > 2\hat{c} + c$, there exists a constant ϵ_3 so that if $\epsilon \in (0, \epsilon_3)$, then $c_e \ge 2\hat{c} + r\epsilon + c$. Let $\epsilon^* = \min\{\epsilon^*_2, \epsilon_3\}$. If $\epsilon \in (0, \epsilon^*)$ and $c_e \ge c_{e_1} + c$, then $V_v(t) \le c_e$ for $t \in [t_0 + T_1(\epsilon), t_0 + T_3)$ and hence $\frac{1}{2}\boldsymbol{e}(t)^\top \boldsymbol{P}_m \boldsymbol{e}(t) \le c_e$ for $t \ge t_0 + T_1(\epsilon)$, which implies that $T_3 \to \infty$. Because $\boldsymbol{e}(t) \in \boldsymbol{\Omega}_e$ for $t \in [t_0, t_0 + T_1(\epsilon)]$, we have $\boldsymbol{e}(t) \in \boldsymbol{\Omega}_e$ and $\boldsymbol{x}(t) \in \boldsymbol{\Omega}_x$ for $t \ge t_0$.

It follows from Theorem 1 and the above analysis that $V_v(t)$ will visit the interval $[0, 2\hat{c} + r\epsilon]$ infinitely often for $t \ge t_0+T_1(\epsilon)$. Let $T \ge t_0+T_1(\epsilon)$ be the first time such that $V_v(T) \le 2\hat{c} + r\epsilon$. The trajectory of $V_v(t)$ starting at $t = T$ will stay inside the interval $[0, 2\hat{c}+r\epsilon]$ until it jumps outside when the controller switches the mode. However, the jump of $V_v(t)$ between different modes satisfies the condition, $|\Delta| \le c$. Hence, we have $V_v(t) \le 2\hat{c} + r\epsilon + c$, which implies that

$$\frac{1}{2}\boldsymbol{e}(t)^\top \boldsymbol{P}_m \boldsymbol{e}(t) \le 2\hat{c} + r\epsilon + c$$

for $t \ge T$. If, in addition, there exists a finite time $T_s \ge t_0 + T_1(\epsilon)$ such that $v = v_s$ for $t \ge T_s$, then it follows from (26) that $\dot{V}_{v_s} \le -\mu_m V_{v_s} - \mu_m(V_{v_s} - 2\hat{c} - r\epsilon)$ for $t \ge T_s$. Thus, there exists a finite time $T \ge T_s$ such that

$$\frac{1}{2}\boldsymbol{e}^\top(t)\boldsymbol{P}_m \boldsymbol{e}(t) \le 2\hat{c} + r\epsilon$$

for $t \ge T$. The proof of the theorem is complete. ■

Remark 2: It can be seen from (28) and (29) that the tracking performance is directly proportional to the magnitude of c, ν and ϵ. Recall that the magnitude of c is inversely proportional to κ. Therefore, large κ and small ν and ϵ yield better tracking performance.

VI. Simulation Example

We illustrate the effectiveness of the proposed variable neural adaptive robust output feedback controller on the model of the planar articulated two-link manipulator used in [15]. Detailed model derivation of this two-link manipulator can be found in [20, p. 394]. Let q_1 and q_2 denote the angular positions of joint 1 and 2, respectively, and τ_1 and τ_2 denote the applied torques. We assume that there exist input disturbances η_1 and η_2 associated with the applied torques τ_1 and τ_2, respectively. Thus, we can represent the dynamics of this two-link manipulator as

$$\begin{aligned}&\begin{bmatrix} H_{11} & H_{12} \\ H_{21} & H_{22} \end{bmatrix}\begin{bmatrix} \ddot{q}_1 \\ \ddot{q}_2 \end{bmatrix} \\ &\quad + \begin{bmatrix} -h\dot{q}_2 & -h\left(\dot{q}_1 + \dot{q}_2\right) \\ h\dot{q}_1 & 0 \end{bmatrix}\begin{bmatrix} \dot{q}_1 \\ \dot{q}_2 \end{bmatrix} = \begin{bmatrix} \tau_1 + \eta_1 \\ \tau_2 + \eta_2 \end{bmatrix},\end{aligned}$$

where $H_{11} = a_1 + 2a_3\cos(q_2) + 2a_4\sin(q_2)$, $H_{12} = H_{21} = a_2 + a_3\cos(q_2) + a_4\sin(q_2)$, $H_{22} = a_2$ and $h = a_3\sin(q_2) -$

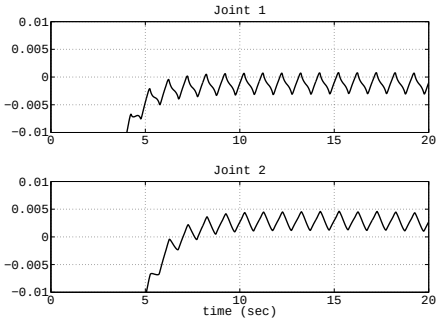

Fig. 1. Output tracking errors (rad).

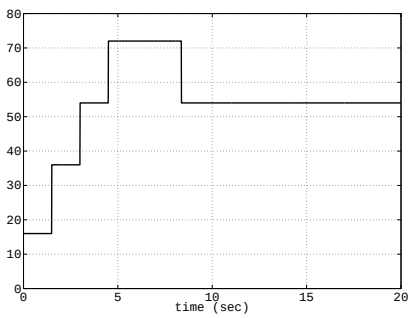

Fig. 2. Variation of the number of grid nodes.

$a_4 \cos(q_2)$ with $a_1 = I_1 + m_1 l_{c1}^2 + I_e + m_e l_{ce}^2 + m_e l_1^2$, $a_2 = I_e + m_e l_{ce}^2$, $a_3 = m_e l_1 l_{ce} \cos(\delta_e)$ and $a_4 = m_e l_1 l_{ce} \sin(\delta_e)$. In our simulation, we use the same numerical values as in [20, p. 396], that is, $m_1 = 1.0$ (kg), $m_e = 2.0$ (kg), $I_1 = 0.12$ (kg·m^2), $I_e = 0.25$ (kg·m^2), $l_{c1} = 0.5$ (m), $l_{ce} = 0.6$ (m), $l_1 = 1$ (m) and $\delta_e = \pi/6$ (rad). We also use the band-limited white noise signals for the input disturbances η_1 and η_2 as in [15]. The manipulator is initially at rest, that is, $q_1 = q_2 = 0$ and $\dot{q}_1 = \dot{q}_2 = 0$.

We consider the same reference signals as in [11], that is, $q_{d1}(t) = \frac{\pi}{6}\cos(2\pi t)$ and $q_{d2}(t) = \frac{\pi}{4}\cos(2\pi t)$. Thus, we choose the grid boundaries for q_1, $\dot{q}_1$, q_2 and $\dot{q}_2$ to be $[-1.0\ \ 1.0]$, $[-4.0\ \ 4.0]$, $[-1.0\ \ 1.0]$ and $[-5.5\ \ 5.5]$, respectively. For the controller, we choose $\boldsymbol{k}_1 = [1\ 2]$, $\boldsymbol{k}_2 = [4\ 4]$, $\boldsymbol{Q}_1 = \boldsymbol{Q}_2 = 0.5\boldsymbol{I}_2$, $d_f = d_g = d_o = 5$, $\nu = 0.025$, $\underline{g} = 0.1$ and $\boldsymbol{G}_0 = 2\boldsymbol{I}_2$. The remaining design parameters of the variable-structure RCRBF network are: $e_{\max} = 0.005$, $\rho = 0.8$, $\varrho = 0.3$, $\boldsymbol{d}_{\text{threshold}} = [0.1\ 0.4\ 0.1\ 0.55]$, $\underline{\omega}_1 = \underline{\omega}_2 = -25$, $\overline{\omega}_1 = \overline{\omega}_2 = 25$, $\kappa = 500$ and $T_d = 1.5$. For the high-gain observer, we select $\alpha_{11} = \alpha_{21} = 2$, $\alpha_{12} = \alpha_{22} = 1$ and $\epsilon = 10^{-4}$. In addition, we select $U_1 = 250$ and $U_2 = 150$. It can be seen from Fig. 1 that the trajectories of the output tracking errors enter a small neighborhood around the origin and then stay there thereafter. The variation of the number of hidden neurons is shown in Fig. 2. When the tracking performance is poor, the network adds more RBFs in order to improve the approximation accuracy. When the tracking performance is acceptable, the network removes RBFs in order to avoid network redundancy.

VII. Conclusions

A variable neural adaptive robust output feedback controller has been proposed for the output tracking control of a class of MIMO uncertain systems. The variable-structure RBF network, which is used to approximate unknown system dynamics, can grow or shrink on-line dynamically according to the tracking performance. The piecewise quadratic Lyapunov function is utilized to analyze the effects of the structure variation of the RBF network. Simulation results confirm the effectiveness of the proposed variable neural adaptive robust output feedback controller.

References

[1] I. Kanellakopoulos, P. V. Kokotovic, and R. Marino, “An extended direct scheme for robust adaptive nonlinear control,” *Automatica*, vol. 27, no. 2, pp. 247–255, 1991.

[2] A. Kojic and A. M. Annaswamy, “Adaptive control of nonlinearly parameterized systems with a triangular structure,” *Automatica*, vol. 38, no. 1, pp. 115–123, 2002.

[3] M. Krstić and P. V. Kokotović, “Adaptive nonlineaer design with controller-identifier separation and swapping,” *IEEE Trans. Autom. Control*, vol. 40, no. 3, pp. 426–460, Mar. 1995.

[4] E. B. Kosmatopoulos and P. A. Ioannou, “Robust switching adaptive control of multi-input nonlinear systems,” *IEEE Trans. Autom. Control*, vol. 47, no. 4, pp. 610–624, Apr. 2002.

[5] R. M. Sanner and J. J. E. Slotine, “Gaussian networks for direct adaptive control,” *IEEE Trans. Neural Netw.*, vol. 3, no. 6, pp. 837–863, Nov. 1992.

[6] A. Yesildirek and F. L. Lewis, “Feedback linearization using neural networks,” *Automatica*, vol. 31, no. 11, pp. 1659–1664, 1995.

[7] S. Seshagiri and H. K. Khalil, “Output feedback control of nonlinear systems using RBF neural networks,” *IEEE Trans. Neural Netw.*, vol. 11, no. 1, pp. 69–79, Jan. 2000.

[8] C.-C. Liu and F.-C. Chen, “Adaptive control of non-linear continuous-time systems using neural networks—general relative degree and MIMO cases,” *Int. J. Contr.*, vol. 58, no. 2, pp. 317–335, 1993.

[9] Y.-C. Chang, “An adaptive H$^\infty$ tracking control for a class of nonlinear multiple-input-multiple-output (MIMO) systems,” *IEEE Trans. Autom. Control*, vol. 46, no. 9, pp. 1432–1437, Sep. 2001.

[10] S. Tong and H.-X. Li, “Fuzzy adaptive sliding-mode control for MIMO nonlinear systems,” *IEEE Trans. Fuzzy Syst.*, vol. 11, no. 3, pp. 354–360, Jun. 2003.

[11] H. Xu and P. A. Ioannou, “Robust adaptive control for a class of MIMO nonlinear systems with guaranteed error bounds,” *IEEE Trans. Autom. Control*, vol. 48, no. 5, pp. 728–742, May 2003.

[12] H. K. Khalil, “Adaptive output feedback control of nonlinear systems represented by input–output models,” *IEEE Trans. Autom. Control*, vol. 41, no. 2, pp. 177–188, Feb. 1996.

[13] G. P. Liu, V. Kadirkamanathan, and S. A. Billings, “Variable neural networks for adaptive control of nonlinear systems,” *IEEE Trans. Syst., Man, Cybern. B*, vol. 39, no. 1, pp. 34–43, Feb. 1999.

[14] J. Lian, Y. Lee, and S. H. Żak, “Variable neural direct adaptive robust control of uncertain systems,” *IEEE Trans. Autom. Control*, vol. 53, no. 11, pp. 2658–2664, Dec. 2008.

[15] J. Lian, J. Hu, and S. H. Żak, “Adaptive robust control: A piecewise Lyapunov function approach,” in *Proc. American Control Conference*, St. Louis, MS, Jun. 2009, pp. 568–573.

[16] M. S. Branicky, “Multiple Lyapunov functions and other analysis tools for switched and hybrid systems,” *IEEE Trans. Autom. Control*, vol. 43, no. 4, pp. 475–482, 1998.

[17] M. Johansson and A. Rantzer, “Computation of piecewise quadratic Lyapunov functions for hybrid systems,” *IEEE Trans. Autom. Control*, vol. 43, no. 4, pp. 555–559, Apr. 1998.

[18] N. A. Mahmoud and H. K. Khalil, “Asymptotic regulation of minimum phase nonlinear systems using output feedback,” *IEEE Trans. Autom. Control*, vol. 41, no. 10, pp. 1402–1412, Oct. 1996.

[19] F. Esfandiari and H. K. Khalil, “Output feedback stabilization of fully linearizable systems,” *Int. J. Contr.*, vol. 56, no. 5, pp. 1007–1037, 1992.

[20] J.-J. Slotine and W. Li, *Applied Nonlinear Control*. Englewood Cliffs, NJ: Prentice Hall, 1991.